RESIDUAL STRESSES IN BULK METALLIC GLASSES DUE TO DIFFERENTIAL COOLING OR THERMAL TEMPERING

E. USTUNDAG[†], B. CLAUSEN*, J. C. HANAN[†], M. A. M. BOURKE*, A. WINHOLTZ[‡‡] and A. PEKER[†]**
[†]California Institute of Technology, Department of Materials Science, M/C 138-78, Pasadena, CA 91125; ustundag@hyperfine.caltech.edu
*Los Alamos National Laboratory, LANSCE, MS H805, Los Alamos, NM 87545
[‡‡]Research Reactor Center, Research Park, University of Missouri, Columbia, MO 65211
**Amorphous Technologies, 27722 El Lazo, Laguna Niguel, CA 92677

ABSTRACT

Due to their very low thermal conductivities and large thermal expansion values, bulk metallic glasses (BMGs) undergo differential cooling during processing. Large thermal gradients are generated across a specimen leading to residual stress buildup. A thin surface layer contains compressive stresses balanced by tension in the middle. Such stresses can not only influence the mechanical behavior of BMGs, but they can also lead to problems during manufacturing of large or intricate components. Analytical and finite element modeling was used to predict the values and distribution of such stresses as a function of processing conditions. Neutron diffraction measurements were then performed on model specimens which included crystalline phases as "strain gages". It was shown that significant stresses, on the order of several hundred MPa, can be generated in BMGs. Modeling and diffraction results are presented and their implications discussed.

INTRODUCTION

Although metallic glasses have been made since 1960s, specimen dimensions were previously limited to tens of μm due to the very fast cooling rates (about 10^6 K/s) needed in order to prevent crystallization in most systems. Recently, multicomponent alloys have been developed with exceptional glass formation ability that allow the processing of *bulk* specimens. One of the most successful bulk metallic glass (BMG) alloy series (Zr-Ti-Cu-Ni-Be) has been developed at Caltech [1]. These alloys form metallic glasses at cooling rates as low as 1 K/s allowing the casting of specimens up to 5 cm in diameter while still retaining the glassy structure. The ability to prepare large specimens has permitted the bulk characterization of these materials using more "traditional" techniques. The unique properties of BMGs potentially place them among significant engineering materials: very high strength (up to 1.9 GPa) and initiation fracture toughness (40-55 MPa.$m^{1/2}$), a near theoretical specific strength, excellent wear and corrosion resistance, high elastic strain limit (up to 2%), and so on [2, 3].

The properties of BMGs are influenced by, among other parameters, residual stresses. A potentially major source of such stresses is differential cooling. The cooling rates currently used to process large specimens are still fast enough to lead to large thermal gradients inside BMGs. This is magnified by their extremely poor thermal conductivity ($k \approx 4$ W/m-K, compared to ~400 W/m-K for Cu) which leads to a rapid cooling of the outside while the middle is still well above the glass transition temperature. Additional factors such as rapid variation of viscosity [4] and coefficient of thermal expansion (CTE) [5] with temperature can also add to this effect leading to potentially very high residual stresses [6, 7]. The result is an effect called 'thermal tempering' as is seen in silica-based glasses where a surface layer with compressive stresses is balanced with a tensile stress in the middle [8, 9, 10, 11]. Such a stress state significantly increases the fracture and impact resistance of silica glass due to inhibition of surface cracks.

BMGs have, in principle, a higher potential in tempering due to their higher strength and CTE values. Indeed, as it will be shown by our preliminary calculations and measurements, residual stresses of up to 900 MPa can be generated due to this process (silica glass would usually be tempered with

Mat. Res. Soc. Symp. Proc. Vol. 554 © 1999 Materials Research Society

surface stresses around 100-150 MPa [8]). Such high stresses are expected to have profound effects on material properties as well as processing conditions. This paper presents the preliminary results of a systematic study to identify mechanisms that influence tempering stress generation and relaxation in BMGs, to measure these stresses using neutron diffraction and compare the results to analytical and finite element calculations.

BACKGROUND

Residual stress generation due to rapid cooling, sometimes referred to as *thermal tempering*, is a well known phenomenon in metals and silica glasses. Despite its high potential for significant stress buildup, however, this topic has received little attention in metallic glasses. Almost all studies noted in literature investigated the tempering stresses in magnetic metallic glass ribbons (see for example [12, 13]). The thrust of this work was the determination of the effect of internal stresses on the magnetic domain structure of these materials due to the magnetoelastic effect. Among the noteworthy results of these studies is the measurement of residual compressive stresses of about 100 MPa despite the use of very thin (30-40 μm) ribbons. This is another demonstration of the potential of internal stress generation due to rapid cooling in metallic glasses. On the other hand, no systematic tempering stress studies are known on *bulk* metallic glasses where these stresses are potentially higher due to large specimen dimensions.

The tempering of silica glass, in turn, is an extensively studied topic. It has been known since the demonstration of the so-called Prince Rupert drops in the 17th century, but more systematically since 1891 when the Schott's process was introduced, that glass can be treated to achieve high strength and impact resistance [14]. There are a number of methods to strengthen silica glass, e.g., via chemical means [14], but here only the thermal methods will be reviewed briefly due to their direct relevance to the metallic glass case.

The tempering of silica glass involves rapid quenching from a temperature above its strain point. During this process, surface cools more rapidly than the interior, and in a few seconds a large thermal gradient is attained. Then the interior cools more rapidly than the surface until room temperature is reached. Initially, therefore, the thermal contraction of the surface is greater than that of the midplane. This differential contraction tends to produce tensile stresses on the surface and compressive stresses in the interior. In an elastic solid these stresses would be cancelled by stresses of opposite sign during the later stage of quenching, in which the cooling rate of the midplane exceeds that of the surface. However, since glass is a viscoelastic material with rapidly varying viscosity as a function of temperature, the initial stresses are relaxed at high temperatures. On the other hand, the stresses generated later, by the contraction of the middle, are not relaxed leading to residual compressive stresses balanced by interior tension [8].

THEORETICAL CALCULATIONS OF TEMPERING STRESSES

Analytical Calculation

A simple calculation was performed adapting an analytical model developed for silica glass tempering [15] called the 'Instant Freezing Model'. The model was later modified by Indenbom and Vidro [16]. It assumes that the material is a perfect fluid above the glass transition temperature, T_g, incapable of supporting any stresses and a perfectly elastic solid with no stress relaxation below it. Obviously this is a gross oversimplification considering the continuous albeit fast variation of material properties around this temperature. However, it has been shown that predictions of the model are reasonably close to measured stress values although information about transient effects is lost [8].

In this calculation [6] the room-temperature values of BMG elastic constants (E = 90 GPa, ν = 0.35) were used as well as T_g = 625 K, final temperature, T_a = 298 K and $k \approx 4$ W/m-K. Since specimens are usually quenched in water after casting, heat transfer coefficients were chosen to correspond to laminar and turbulent water flow over sample surface: h = 2000 W/m^2.K for the former and h = 10000

W/m^2.K for the latter [17]. In the 'Instant Freezing Model' midplane tension, σ_M, of an *infinite plate* is given by [15, 16]:

$$\sigma_M = \frac{\beta E}{1-\nu}(T_g - T_a)\left(1 - \frac{\sin\delta_1}{\delta_1}\right) \qquad (1)$$

where, β is the CTE and δ_1 is the first root of $\delta \tan(\delta) = ht/k$ (Biot number), and t is the half thickness of the plate. The surface stress is then calculated from $\sigma_S = -\sigma_M f(t)$ where $f(t)$ is a function of the thickness and the Biot number and takes values between 2 and 5.

The calculated surface compressive stresses for each cooling case are shown in Fig. 1. There is about 200 MPa difference in compressive stress values between the laminar and turbulent flow cases for a given half thickness. In either case, it is seen that very high compressive stress values can be obtained due to tempering, e.g. up to 900 MPa for a half thickness of 2 cm, a dimension easily accessible with the current BMG processing techniques.

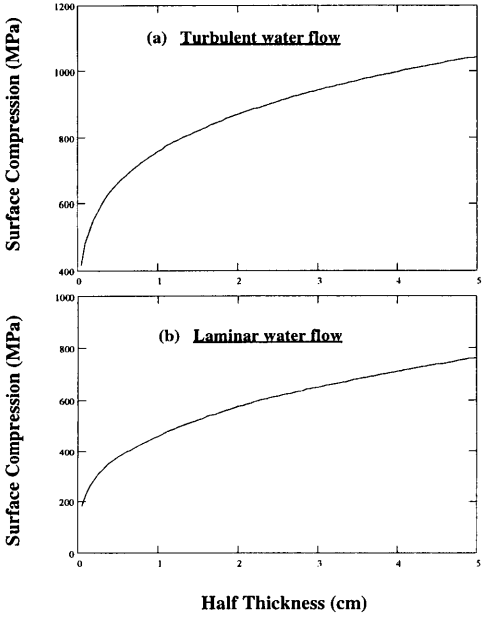

Figure 1. Surface stresses in an infinite plate predicted by the "Instant Freezing Model'.

Finite Element Modeling

The finite element (FE) calculations of the two geometries chosen as model specimens (and described later) were made using ABAQUS (version 5.7) in the standard non-linear implicit mode. The full details of the calculation will be presented elsewhere [6]; here only one of the specimens is discussed for brevity. The FE model is axis-symmetric; hence, only a quarter of a plane along the cylinder axis was taken into account. A heat flux through the top and right hand side of the model was applied to simulate the cooling in water. As a typical assumption used in FE models, the interfaces were regarded as perfect, which in this case is a realistic assumption. Coupled temperature and displacement calculations were used to determine the transient stresses and strains in the sample. The element size was biased so the smallest elements were at the top surface and at the interfaces.

The stainless steel (SS) used in the model specimens was assumed to be an elastic-plastic material with linear strain hardening, while the BMG was modeled as a viscoelastic material. Some approximations were made for the viscoelastic properties, as these properties are not yet available for BMG. Namely, the shape of the curve that describes the relaxation of stresses as a function of time at a given temperature (in the form of a Prony series in ABAQUS [18]) was taken to be that of silica glass [11]. It is difficult to estimate the errors introduced by using these adapted material data. However, the functional form of the relaxation curve is the same for all viscoelastic materials which should ensure that only the numerical values of the stresses and strains calculated using these parameters are subjected to errors, but the general trends should be well described by the model. The cooling rate was assumed to be that of laminar water flow, similar to the case with the analytical model. Another important variable in tempering, the initial temperature, was taken to be around 670 K (close to the glass transition temperature

of BMG) although the casting of the model specimens was done at 1173 K. Since a higher initial temperature is predicted to lead to larger tempering stresses (based on the silica glass data [8]), the current version of the FE model should be viewed as an underestimate. Furthermore, the thermal conductivity ($k \approx 16$ W/m-K) of type 314 SS used is much lower than that of Cu normally used in the casting molds for BMG. For this reason, the model specimen shown in Fig. 2 is not optimized in terms of tempering stresses.

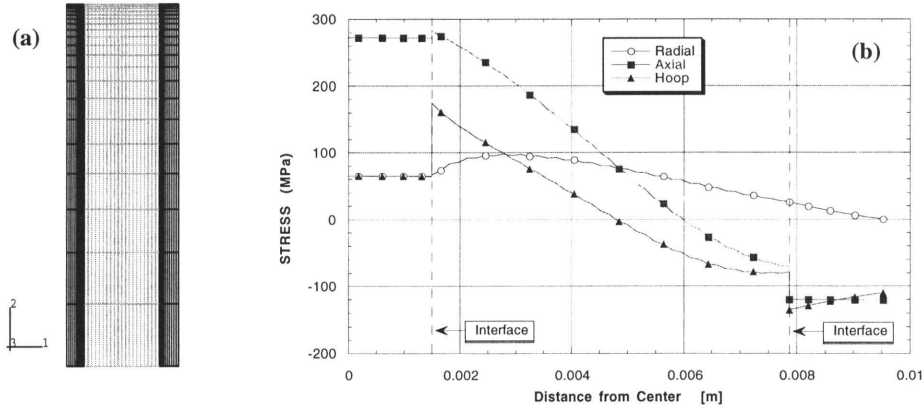

Figure 2. Finite element model (a), and calculated residual stress distribution due to tempering in a model specimen (b). The dark lines in (a) indicate the stainless steel regions; the rest is BMG.

Nevertheless, the stresses predicted are still substantial. The stress distribution shown in Fig. 2(b) follows the predictions of the tempering theory. The middle of the sample is under high tension and the surface is compressed. In the FE model, three different calculation schemes were assumed (details are reported elsewhere [6]). The FE model predictions for each case are shown in Fig. 3.

Scenario 1: only CTE mismatch between SS and BMG (both materials are elastic);

Scenario 2: Scenario 1 plus viscoelasticity in BMG;

Scenario 3: all the above plus plasticity in SS.

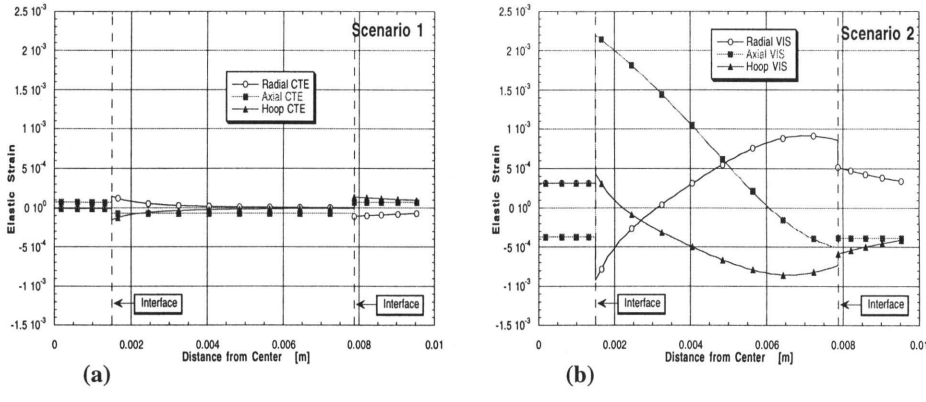

Figure 3. Finite element model predictions of *elastic strain* components for each calculation scenario. The specimen geometry is depicted in Fig. 2(a).

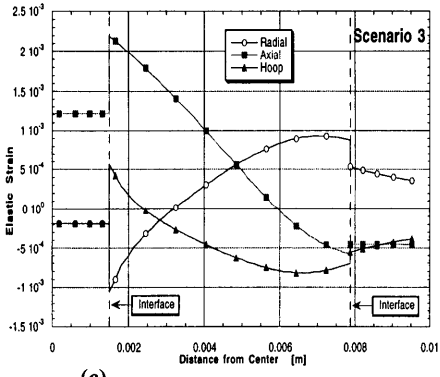

(c) **Figure 3.** Continued.

It is seen that only the introduction of viscoelasticity in BMG (Scenario 2) leads to a substantial, and more 'realistic' change in the strain state. The average residual strains in *steel* are shown in Table I. Despite some relaxation by yielding in this region, the residual stresses predicted are still quite appreciable.

EXPERIMENTAL

Sample Preparation

The specimen shown in Fig. 2 was prepared by casting a BMG alloy (Vitreloy 1: $Zr_{41.2}Ti_{13.8}Cu_{12.5}Ni_{10}Be_{22.5}$) in a long, type 314 stainless steel (SS) tube (19.0 mm outer diam., 15.6 mm inner diam.) at 1173 K after which it was dropped in water at room temperature for quenching. Other details of specimen preparation were presented elsewhere [1]. The tube had a welded pin (3.2 mm diam.) in its middle intended to provide 'contrast' in the strain state due to tempering. Both interfaces were observed to be intact after processing. A 50 mm long section of the BMG/SS composite structure was cut for strain measurements. An identical tube (with an attached pin) was also heat treated under the same conditions, but without a BMG core, to be used as a stress-free reference. The primary function of the SS components was to serve as 'strain gages' in neutron diffraction strain measurements.

Table I: Calculated and measured *average* elastic strain components in steel in the model sample (Fig. 2)

Strain Component	*Measured*	Calculated, scenario 1	Calculated, scenario 2	*Calculated, scenario 3*
Axial, pin	1420×10^{-6}	72×10^{-6}	-385×10^{-6}	1210×10^{-6}
Axial, tube	-137×10^{-6}	72×10^{-6}	-375×10^{-6}	-454×10^{-6}
Radial, tube	847×10^{-6}	-92×10^{-6}	314×10^{-6}	500×10^{-6}

Neutron Diffraction Strain Measurements

Some preliminary strain measurements in the model sample were performed at the Missouri University Research Reactor (MURR). These were made using a monochromatic neutron beam of 1.478 Å on the 2XD powder diffractometer. The (311) stainless steel peak at 86.6° (2θ) was employed. The gage volume for the measurements, defined by a 4 inch long 1x8 mm boron nitride incident beam collimator and a 1 mm cadmium slit on the diffracted beam, was almost a perfect rectangular box (a 1x1x8 mm "match stick").

DISCUSSION

The neutron strain measurement results and their comparison to the three different finite element models are shown in Table I. There is a very close correspondence between experimental data and the model predictions by the third scenario. This is encouraging although the model is still very preliminary and has not been optimized [6]. The occurrence of tempering can be concluded, for instance, from a comparison between the first and third scenarios. If only the CTE mismatch were the source of residual stresses, then the first case should have applied. However, the presence of the viscoelasticity in BMG leads to tempering. At this stage, these residual stresses are not optimized. The relatively poor thermal

conductivity of SS prevented the realization of faster cooling. In any case, it should be noted that the SS/BMG assembly is already a tempered product with appreciable compressive stresses in the SS tube.

SUMMARY

The viscoelastic nature of BMGs, their poor thermal conductivity and the fast cooling utilized in their processing lead to thermal tempering; namely, compressive stresses on the surface and tension in the interior. Both a simple analytical calculation and finite element models predict substantial residual stress generation in BMGs due to this effect (up to 900 MPa on the surface). Preliminary neutron diffraction strain measurements on model specimens support this and point to a potential of significant property manipulation via such residual stresses. A systematic study is underway that involves modeling and experimentation to investigate stress generation/relaxation mechanisms in BMGs and to quantify the effect of these stresses on their properties.

REFERENCES

1. A. Peker and W. L. Johnson, *Appl. Phys. Lett.*, **63**, 2342 (1993).
2. C. J. Gilbert, R. O. Ritchie and W. L. Johnson, *Appl. Phys. Lett.*, **71** (4), 476 (1997).
3. H. A. Bruck, T. Christman, A. J. Rosakis and W. L. Johnson, *Scripta Metall.* **30**, 429 (1994).
4. E. Bakke, R. Busch and W. L. Johnson, *Appl. Phys. Lett.*, **67** (22), 3260 (1995).
5. K. Ohsaka, S. K. Chung, W. K. Rhim, A. Peker, D. Scruggs and W. L. Johnson, *Appl. Phys. Lett.*, **70** (6), 726 (1997).
6. B. Clausen, E. Üstündag, J. C. Hanan and M. A. M. Bourke, *in preparation* (1998).
7. B. Clausen, E. Üstündag and M. A. M. Bourke, *in preparation* (1998).
8. R. Gardon in *Glass Science and Technology, vol. 5: Elasticity and Strength in Glasses,* edited by D. R. Uhlmann and N. J. Kreidl, pp. 146-216, Academic Press, New York, 1980.
9. O. S. Narayanaswamy and R. Gardon, *J. Am. Ceram. Soc.*, **52** (10), 554 (1969).
10. O. S. Narayanaswamy *J. Am. Ceram. Soc.*, **54** (10), 491 (1971).
11. H. Carre and L. Daudeville, *J. de Phys. IV*, vol. **6**, 175, (1996).
12. M. de Jong, J. Sietsma, M. Th. Rekveldt and A. van den Beukel, *Mat. Sci. and Eng.*, **A179-A180**, 341 (1994).
13. M. Tejedor, J. A. Garcia, J. Carrizo and L. Elbaile, *J. Mater. Sci.*, **32**, 2337 (1997).
14. R. F. Bartholomew and H. M. Garfinkel, in *Glass Science and Technology, vol. 5: Elasticity and Strength in Glasses,* edited by D. R. Uhlmann and N. J. Kreidl, pp. 217-270, Academic Press, New York, 1980.
15. Z. M. Bartenev, *Zh. Tekhn. Fiz.*, **19** (12), 1423 (1949).
16. V. L. Indenbom and L. I. Vidro, *Sov. Phys. Solid State*, **6** (4), 767 (1964).
17. S. Yanniotis and D. Kolokotsa, *J. of Food Eng.*, **30** (3-4) 313 (1996).
18. ABAQUS Theory Manual, Hibbitt-Karlsson-Sorensen, Inc., Pawtucket, RI, 1995.